Cell fusion proteins can rejuvenate adult dendritic trees

Veronika Kravtsov[1,#], Meital Oren-Suissa[1,2,#], and Benjamin Podbilewicz[1†]

[1]Department of Biology, Technion- Israel Institute of Technology, Haifa 32000, Israel

[#]These authors contributed equally to this work

[†]Correspondence to: podbilew@technion.ac.il

Additional footnotes:

[2]Present address: Columbia University Medical Center, Department of Biochemistry & Molecular Biophysics, New York, 10032, USA

Abstract

The convoluted architecture of dendritic arbors poses a challenge to understanding age-dependent alterations and regeneration following injury. Here, we show that induction of cellular fusogens can remodel and facilitate regeneration of dendrites in polymodal PVD neurons of aging *Caenorhabditis elegans*. Using whole-animal live imaging, we find that the PVD dendritic trees, composed of repetitive "menorah" units, show age-dependent hyperbranching, disorganization, and loss of self-avoidance. These processes, while independent of canonical lifespan-regulating pathways, can be partially rescued by ectopic expression of the fusogen EFF-1. Furthermore, the decreased capacity of old animals to repair laser-induced severed dendrites via auto-fusion can be restored by reducing DAF-2 (Insulin/IGF-1Receptor) function or by ectopic expression of the EFF-1 paralog AFF-1. Our findings demonstrate that fusogens are sufficient to maintain the dendritic arbor structure and increase its regeneration potential in aging animals. These antiaging strategies can be potentially applied to other organisms to protect them from neurodegeneration.

Introduction

Aging is the primary risk for neuronal diseases and general cognitive decline in humans [1], yet, our understanding of the process of neuronal aging at the molecular and cell biological levels is still limited. In particular, very few studies have investigated the fate of complex dendritic arbors during aging, and their regenerative capacity following injury. *C. elegans* is a powerful system to study the genetics of neuronal aging and regeneration [2-4]. Signaling via the DAF-2 Insulin/IGF-1 receptor is the most prominent and conserved pathway that controls aging and longevity of *C. elegans*, flies, and mammals [2]. Normally, when the DAF-2/IGF-1 receptor is activated it induces a conserved PI3K/AKT kinase cascade, which in turn inhibits the DAF-16/FOXO transcription factor from entering into the nucleus. Reduction of *daf-2*

42 function doubles life span, and long-lived worms are considered to stay healthy for longer [2,5].
43 In these animals, DAF-16/FOXO affects transcription of different genes that encode heat-
44 shock proteins, antimicrobial proteins, antioxidants, and other molecules, which leads
45 ultimately to extended lifespan [6,7]. Recently, aging-associated axonal morphological
46 alterations and decline in regenerative capacity were described in *C. elegans*. *daf-2*
47 mutations delayed these age-related morphological changes and improved regeneration of
48 aged severed axons in a *daf-16*-dependent manner [8-11]. Moreover, in the case of GABA
49 motor neurons, as adult animals age there is a reduction in axon growth, retraction and
50 regrowth in response to injury. Surprisingly, the decline in regeneration is controlled by *daf-*
51 *16* in a cell-autonomously fashion and independently of lifespan [11].
52 Different invertebrates, including nematodes and crustaceans, use membrane fusion as
53 an alternative mechanism for repair of injured axons [12-15]. Cell fusion events were also
54 observed in the brains of mammals both spontaneously and as a result of injury such as stroke
55 [16-18], but the role of these events has remained unclear. In *C. elegans*, axonal regeneration via
56 auto-fusion is mediated by the fusogen EFF-1 [12,13,15]. EFF-1 is the first *bona fide* eukaryotic
57 developmental cell-cell fusion protein. It is expressed in different cell types including
58 neurons, and mediates fusion between cells by a homotypic mechanism [19-21].
59 We have been studying the role of fusion proteins in the PVD neuron, a polymodal
60 nociceptor that senses harsh touch to the body, cold temperature, and proprioception [22-25].
61 The PVD neuron exhibits an elaborate and invariant network of dendrites, which is composed
62 of a repetitive unit that is termed "menorah" **(Figure 1A)** [23]. Menorahs arise and are
63 maintained through several intrinsic and extrinsic genetic pathways [23-33].
64 The PVD develops in a stereotypic fashion from the L2 larval stage to the young adult
65 [23]. The fusion protein EFF-1 mediates dendrite retraction and auto-fusion of excess branches
66 by a novel cell-autonomous pruning mechanism [23]. Thus, this fusogen maintains the

67 menorah structure by trimming excess branching during normal developmental arborization
68 [23]. AFF-1, a paralog of EFF-1, is a second *C. elegans* fusogen displaying a more restricted
69 tissue distribution pattern [34]; AFF-1 was not found to be involved in PVD remodeling during
70 development [35]. AFF-1 and EFF-1 fusion proteins also auto-fuse epithelial and myoepithelial
71 cells to form tubes and reshape glial cells [36-38]. Moreover, it has recently been demonstrated
72 that in vertebrates auto-fusion takes place in the development of the vascular endothelium,
73 where it leads to pruning of excess blood vessels [39] in a process that remarkably resembles
74 EFF-1-mediated PVD pruning [23]. It is unknown whether PVD structure and function is
75 affected by aging and by the activity of fusion proteins.
76 Here, we use the PVD polymodal neuron as a model to study how aging affects the
77 morphology, function, and regeneration of dendrites following injury. Our study
78 demonstrates the age-related progressive morphological alterations of intricate dendritic
79 arbors in a living organism. We found that the fusogen EFF-1, when expressed in the PVD
80 neuron, simplifies and therefore rejuvenates aged dendritic trees. In contrast, insulin/IGF-1
81 receptor mutations (*daf-2*) fail to inhibit the progressive aging of dendrites and do not prevent
82 the decline in response to harsh touch during aging. We also discovered that PVD aging is
83 characterized by a decline in regenerative potential of dendrites following experimental laser
84 dendrotomy. Furthermore, the regeneration of transected dendritic trees can be restored in old
85 animals by DAF-2 insulin/IGF-1 receptor mutations, and can be differentially reestablished
86 by ectopic AFF-1 fusogen expression. Thus, fusogens ectopically expressed in the PVD and
87 mutations in DAF-2/IGF-1R, differentially rejuvenate some aspects of dendritic architecture
88 and regeneration potential in aging *C. elegans*.
89
90

91 **Results**

92

93 **Progressive dendritic remodeling during aging is independent from the Insulin/IGF-1**

94 **pathway**

95 To determine how aging affects the complex arborized dendritic structure, we analyzed the *C.*

96 *elegans* PVD dendritic branching patterns from the fourth larval stage (L4) to ten-day-old

97 adults. We found that during aging PVD's dendrites and menorah structure undergo

98 disorganization and hyperbranching, which is particularly evident in regions closer to the cell

99 body **(Figure 1A and 1C)**. Remarkably, we found that these age-dependent morphological

100 changes of the PVD dendritic pattern were not affected in long-lived animals carrying a

101 mutation in *daf-2* **(Figure 1A-1H, and Figure 1-figure supplement 1)**. Adjacent menorahs

102 normally avoid each other [40], and we found that as the animal ages menorahs lose their self-

103 avoidance properties **(Figure 1C, 1D, and 1I)**. Consistently, this age-dependent dendritic

104 pattern did not improve in *daf-2* mutant animals; young *daf-2* animals at the L4 stage

105 exhibited significantly more *daf-16*-dependent self-avoidance deficiencies in comparison to

106 wild-type **(Figure 2)**. Thus, taken together our results reveal that aging causes a *daf-2*-

107 independent increase in disorganized branching and loss of menorah self-avoidance.

108 To further understand the nature of the age-dependent dendritic tree remodeling, we

109 followed individual animals over time and analyzed time-lapse movies. We found that 5-day

110 adults still exhibited some plasticity of the dendritic tree, with dynamic growth and retraction

111 events **(Figure 3A** and **Movie S1)**; however, both growth and retraction were approximately

112 two times slower **(Figure 3B)** compared to younger L4 animals. To shed more light on the

113 link between structure and function of dendrites during aging, we performed a functionality

114 test. PVD responds to harsh stimulations, and we used a classic harsh touch assay in *mec-4*

115 mutant animals to specifically test PVD activity without the background light touch response

116 mediated by the six light-touch mechanosensory neurons [23,41]. First, we found that although
117 *mec-4* animals have shorter life spans [10], their dendrites looked similar to wild-type between
118 the ages L4-5d **(Figure 4)**, which further demonstrates that the morphological alterations we
119 see are lifespan-independent. Second, we found that the PVD functionality decreased with
120 aging, with 5d adults presenting a reduced harsh touch response in comparison to 1d adults,
121 in both *mec-4* as well as *mec-4;daf-2* double mutants **(Figure 4F)**. The specific components
122 in the PVD circuit affected in 5d adults have not been identified and it is possible that
123 multiple components of the sensorimotor circuit contribute to the age-dependent decline in
124 PVD activities. Thus, our results reveal that the morphological and behavioral hallmarks of
125 aging in PVD dendritic arbors are independent from the canonical IGF-1 pathway that affects
126 lifespan.
127
128 **Age-dependent dendrites remodeling can be modulated by EFF-1**
129 The fusogen EFF-1 is essential to fuse some injured axons in *C. elegans* [12,15], and is involved
130 in PVD's dendrite pruning in a cell-autonomous and dosage-dependent manner during
131 development and in young adults [23]. When EFF-1 is overexpressed in the PVD, a strong
132 gradient of arborization is seen in L4s and young adults, with almost complete lack of
133 branches in areas that are distal from the cell body. However, in areas around the cell body
134 the PVD menorahs appear similar to those in the wild-type [23] **(Figure 5A** and **5B)**. Since
135 EFF-1 retracts and simplifies dendritic arbors in young animals [23] and is expressed in the
136 PVD throughout adulthood (**Figure 5-figure supplement 1**), we hypothesized that EFF-1
137 overexpression will be able to retract dendrites in aged adults. Indeed we found that EFF-1
138 overexpression in the PVDs simplified the hyperbranching around the cell body at 9-10 days
139 adults **(Figure 5C-5E)**; in particular, the quaternary branch order was decreased **(Figure 5F)**.
140 A trend of reduction in fifth and higher order branches also appeared in aged animals

141 overexpressing EFF-1 **(Figure 5G)**. Thus, overexpression of the fusogen EFF-1 in the PVD
142 neuron is sufficient to simplify aged menorahs.
143
144 **Age-dependent decline in dendrite regeneration is dependent on Insulin/IGF-1**
145 Mammalian axons regenerate better in younger individuals than in adults [42]. Similarly, axonal
146 regenerative ability declines drastically as nematodes advance through development and age
147 [11,43]. Our knowledge is still poor on the regenerative capacity of the dendrite, and how aging
148 affects this process of neuronal repair. To study dendritic regeneration we severed the
149 primary dendrites of PVD neuron in aging adults. Typically, the PVDs show robust
150 regeneration at L4 larval stage, consisting in dendrite sprouting from the proximal fragment
151 still attached to the cell body and reconnection via fusion with the separated distal dendrite
152 fragment **(Figure 6A, Movie S2)**. To directly measure reconnection by auto-fusion, we used
153 the photoconvertible reporter Kaede **(Figure 6-figure supplement 1 and Movie S3)**. If
154 fusion fails to occur, the detached distal part eventually degenerates. We found that 2-3 day-
155 old wild-type adults respond more slowly to laser dendrotomy in comparison to L4 and
156 young adults (~70% of the young animals presented regeneration, whereas at the age of 2-3d
157 neither regeneration nor degeneration occurred within 3-6 hours (**Figure 6E and Movie S4)**.
158 At the age of 5 days, the ability to regenerate by dendrite auto-fusion was almost completely
159 lost **(Figure 6C** and **6F)**. Remarkably, long-lived *daf-2* mutants showed similar regeneration
160 to wild-type at L4 stage **(Figure 6B** and **6F)**, whereas at older age (5d) *daf-2* mutants had a
161 much higher regenerative ability than wild-types (70% successful regeneration in *daf-2*
162 versus 12.5% in wild-type) **(Figure 6D** and **6F)**. Similarly to axonal response to injury [11],
163 we found that DAF-2 inhibits regeneration of aged dendrites through inhibition of DAF-16,
164 as *daf-16* mutants and *daf-2;daf-16* double mutants showed regenerative decline during aging
165 similar to wild-type **(Figure 6F)**. In conclusion, our results reveal that dendrite regeneration

166 following transection declines with aging, a phenotype that is dependent on DAF-2/IGF-1R
167 and its target DAF-16/FOXO.
168
169 **AFF-1 mediates and restores dendrite regeneration in aged animals**
170 A second fusogen in *C. elegans* is AFF-1 (Anchor cell Fusion Failure 1), a transmembrane
171 protein related to EFF-1 that executes several fusion events during development [34]. *aff-1*
172 mutants have no evident morphological phenotypes in the PVD neuron and expression has
173 not been detected in the PVD (**Figure 5-figure supplement 1**); moreover, when AFF-1 is
174 ectopically expressed in the PVD in an *eff-1* mutant background it does not retract excess
175 branching, demonstrating that it is unable to rescue the pruning defects of *eff-1* **(Figure 7-**
176 **figure supplement 1)**. However, AFF-1 is required for dendrite fusion in response to injury
177 in L4s and young adults [35]. Adults carrying loss-of-function mutations in *aff-1* have severe
178 egg laying defects, shorter life spans and excretory system defects that prevented us from
179 studying regeneration in aging *aff-1* mutant animals.
180 We next tested whether AFF-1 can restore the regenerative ability of dendrites in
181 older animals by overexpressing AFF-1 specifically in the PVD (PVDp::AFF-1; **Figure 7-**
182 **figure supplement 2**). We found that menorahs of young animals expressing PVDp::AFF-1
183 appeared morphologically wild-type and responded similarly to dendrotomy **(Figure 7A,**
184 **Movie S5)**. However, when 5-day old PVDp::AFF-1 animals were dendrotomized, the
185 percentage of regenerating worms by dendrite fusion was significantly higher compared to
186 wild-type animals (60-80% and 13%, respectively; **Figure 7B and 7C, Movie S6)**.
187 Thus, AFF-1-specific overexpression in the PVD, as well as systemic *daf-2* reduction
188 of function, enables dendrite regeneration in older animals **(Figures 6F and 7C)**.
189

190 **Differential rejuvenation of fusion potential of transected dendrites by *daf-2(-)* and AFF-**
191 **1(+)**
192 We wished to further compare the regenerative modalities of AFF-1 overexpression and *daf-*
193 *2* mutation following dendritic laser-induced severing. Dendritic fusion following injury can
194 occur in three possible ways: 1) tertiary branch fusions that bypass the injury site ("menorah-
195 menorah" fusion); 2) fusion of the proximal primary (1ry) branch to the detached distal 1ry;
196 3) both menorah-menorah fusion and 1ry-1ry fusion **(Figure 8A)**. We found that in wild-
197 type and PVDp::AFF-1 animals at the L4 stage, the most prevalent mechanism of repair is
198 menorah-menorah fusion, whereas in *daf-2* mutants menorah-menorah together with 1ry-1ry
199 fusion (outcome 3) increased compared to wild-type **(Figure 8B-8D)**. In wild-type, we found
200 degeneration in 50% (2-4d) and 80% (5-6d) of the dendrotomized animals **(Figure 8E** and
201 **8H)**. Adult *daf-2* mutant animals (5-6d) presented a response to injury that resembled that
202 observed in L4 wild-type animals, with 70% of the animals showing regeneration, mainly via
203 menorah-menorah fusions **(Figure 8F** and **8I)**. In contrast, in PVDp::AFF-1 animals the
204 response to injury followed a different mechanism, with more regeneration via enhanced 1ry-
205 1ry fusion **(Figure 8G** and **8J)**. However, the AFF-1 effect was unrelated to longevity as
206 PVDp::AFF-1 animals had normal lifespans **(Figure 8-figure supplement 1)**. In summary,
207 rejuvenation of the dendritic arbors uncovered here involves three distinct activities: i) EFF-1
208 pruning of old hyperbranched dendrites, ii) negative regulation of dendrite regeneration by
209 DAF-2/ IGF-1R, and iii) AFF-1-induced auto-fusion of old transected primary dendrites
210 (**Figure 9**).
211
212

213 **Discussion**

214 **Age-related deterioration of dendritic trees is insulin/IGF1-independent**

215 Precise dendritic arborization is critical for proper functioning of neuronal networks, while
216 defective dendritic development and maintenance lead to neuropathologies [44,45]. There is
217 evidence from mammalian CNS showing increase in number and length of terminal dendritic
218 arbors during aging, and reduced arborization in senile dementia [46]. However, it remains
219 unclear whether there is a direct link between altered dendritic structure and reduced function
220 in mammals. Axons of aging neurons also show altered morphologies in diverse species. In
221 *C. elegans* these axonal alterations are not affected by organismal longevity [11,42,43,47]. Here we
222 also found that dendritic alterations during aging are not affected by chronological age;
223 however, unlike the PVD dendrites, in axons the *daf-2* mutation was found to delay the
224 morphological alterations of aged animals [8-10]. Nevertheless, the *daf-2* effect in age-related
225 axonal branching was reported to be uncoupled of its role in extending the lifespan of the
226 worms [8,9]. It thus appears that DAF-2 is specifically involved in cell-autonomous pathways
227 that maintain axonal, but not dendritic morphology. While progressive age-related
228 hyperbranching of the PVD arbors was independent of insulin/IGF-1 pathway,
229 overexpression of EFF-1 in the PVD was sufficient to partially rescue this phenotype in old
230 animals (**Figure 5**). EFF-1 appears to act cell-autonomously to simplify the dendritic trees
231 via its pruning activity mediated by branch retraction [23] (**Figures 5 and 9**).

232

233 **AFF-1 restores regeneration of old broken dendrites via plasma membrane fusion**

234 We further found that dendrite regeneration following PVD dendrotomy decreases with age.
235 This decline was "rescued" in *daf-2* mutants (**Figure 6**). Axonal regeneration is known to
236 decline with age in different organisms [11,42,43,47-49]. In GABA neurons of *C. elegans* the
237 decline in axonal regeneration is also delayed in *daf-2* mutants [11]. However, these neurons do

238 not engage in self-fusion during regeneration, whereas in PVD dendrites the main outcome of
239 regeneration is auto-fusion. Recently, an important role of auto-fusion during axonal
240 regeneration was demonstrated in the PLM sensory neurons of *C. elegans*, a process
241 mediated by the fusogen EFF-1 [12,15]. In the PVD EFF-1 is not necessary for dendrite
242 reconnection following injury [35]. In the PVD dendrites, this role is fulfilled by the EFF-1
243 paralog AFF-1. Significantly, when AFF-1 is ectopically expressed, this fusogen plays a role
244 in maintenance of regenerative potential during aging (**Figures 7 and 9)**. These findings
245 highlight fusion mechanisms as potential target for pharmacological intervention in
246 neuropathologies that result from both injury and aging.
247

248 **Acknowledgments**

249 We thank D. Cassel, M. Hilliard, and A. Sapir for critically reading this manuscript. M.
250 Heiman and C. Yip for providing CHB392, C. Smith and D. Miller for NC1841, and T.
251 Gattegno for BP709. We also want to thank R. Kishony and all members of the Podbilewicz
252 laboratory for discussion. This work was supported by Israel Science Foundation 443/12 and
253 ERC ELEGANSFUSION 268843 grants to BP. Some strains were provided by the CGC,
254 which is funded by NIH Office of Research Infrastructure Programs (P40 OD010440).
255 **Author contributions:** V.K., M.O.S. and B.P. designed the experiments. V.K. performed
256 most experiments. M.O.S. developed the system to study neuronal degeneration and
257 regeneration following dendrotomy using the PVD neurons. M.O.S. generated the
258 PVDp::AFF-1 and PVDp::EFF-1 transgenics and M.O.S. and V.K. tested the effects of EFF-
259 1 and AFF-1 over-expression on regenerating animals. B.P. supervised this work. V.K. and
260 B.P. wrote the paper with input from M.O.S.
261 The authors declare no conflict of interest.
262 This article contains supporting information including six figures and six movies

263 **Materials and Methods**

264

265 **Nematode strains**

266 Animals were maintained at 20°C, unless otherwise stated, according to standard protocols [50].
267 All experiments were performed on hermaphrodites. N2 served as wild-type, and the
268 following mutants and transgenic strains were used:
269 NC1841 *[wdIs52(F49H12.4::GFP); rwIs1(pmec-7::RFP)]* [24], outcrossed 4X, CHB392
270 *[hmnEx133(ser-2prom3::kaede)],* kindly provided by Candice Yip and Max Heiman [51],
271 BP709 *[hmnIs133 (ser-2prom3::kaede)]*, kindly provided by Tamar Gattegno, MF190
272 *[hmIs4(des-2::gfp, pRF4)]* [23]. CB1338 *[mec-3(e1318)IV]*, *Caenorhabditis* Genetics Center
273 (CGC), CB1611 *[mec-4(e1611)X],* (CGC), BP176 *[hyEx23(des-2::eff-1, des-2::gfp, pRF4)]*
274 [23], BP177 *[hyEx392(des-2::eff-1, des-2::gfp, pRF4)],* BP488 *[eff-1(hy21)II; hmIs4;*
275 *hyEx39(des-2p::AFF-1,myo-2::GFP,KS)]*, BP906 *[daf-2(e1370)III; wdIs52; rwIs1],* BP911
276 *[hyEx39; hmnEx133]*, BP915 *[hyEx39; hmnIs133]*, BP551 *[hyEx391(des-2p::AFF-1, myo-*
277 *2::GFP, KS); hmnEx133],* BP919 *[daf-2(e1370)III; daf-16(mu86)I; hmnIs133],* BP923
278 *[daf-16(mu86)I; hmnIs133]*, BP924 *[daf-2(e1370)III; hmnIs133]*, BP925 *[mec-4(e1611)X;*
279 *hmnIs133],* BP926 *[daf-2(e1370)III;mec-4(e1611)X; hmnIs133],* BP1056 *hyEx68[AFF-*
280 *1::TY1::EGFP::3xFLAG, pRF4, KS]; dzIs53[F49H12.4p::mCherry], AFF-*
281 *1::TY1::EGFP::3xFLAG* was kindly provided by transgenome project [52], BP500 *zzIs22*
282 *[pJdC41(eff-1p::EFF-1::GFP), pRF4]; dzIs53 (pF49H12.4::mCherry) zzIs22* was kindly
283 provided by William Mohler [53].

284

285 **Molecular Biology**

286 The *ser-2prom3::Kaede* (pCY2 plasmid) is a kind gift from Candice Yip and Max Heiman [51].
287 It was constructed by digesting *ser-2prom3* with SbfI and AscI and Kaede with AscI and
288 NotI and then ligated together.
289 The *des-2p::AFF-1* construct (pME4 plasmid) was constructed by inserting an AFF-1
290 genomic fragment, digested from *hsp16.2::AFF-1* [34] with NheI and KpnI and cloned into
291 pME2 [23] cut with the same enzymes. *des-2p::AFF-1* was injected at a concentration of 0.1ng/ml
292 into *eff-1(hy21)* animals and three independent lines were obtained. For dendrotomy experiments,
293 two lines (*hyEx39* and *hyEx391*) were crossed into a wild-type background expressing the PVD
294 marker *ser-2p3::Kaede.*
295
296 **Live imaging of worms**
297 Time-lapse imaging and short imaging (one time point) of worms by Nomarski optics and
298 fluorescence microscopy was performed using a Nikon eclipse Ti inverted microscope with
299 Yokogawa CSU-X1 spinning disk or using the Zeiss Laser Scanning Microscope (LSM) 510
300 META. Animals were anesthetized using 0.1% tricaine and 0.01% tetramisole in M9
301 solution for 20-30 minutes, and then they were transferred to a 3% agar slide with an eyelash
302 attached to a toothpick. For short time imaging worms were often mounted on 3% agar slides
303 containing 5–10 mM NaN_3 instead. Image acquisition was done using Andor iQ or
304 Metamorph software, when using the spinning disk confocal (SDC), and Zen software when
305 using the LSM 510 meta microscope. Z-stacks were taken with PlanApochromat 60x oil
306 NA=1.4 objective using the SDC or 63x NA=1.4 objective using the LSM. Excitation of
307 GFP and green Kaede was done with 488 nm wavelength laser and 525 filter (6-15%, 50 ms
308 exposure time), RFP and red Kaede was excited with 561 nm wavelength laser and 607 filter
309 (15-20%, 50-100 ms exposure time). When using the sCMOS (Andor) camera z-stacks were
310 taken with ~0.23 μm z-step. With iXon EMCCD camera (Andor) z-stacks were taken with

311 ~0.5 μm z- step, gain was ~100. When the LSM 510 meta was used, z-step was ~0.8 μm.
312 Multidimensional data was reconstructed as maximum intensity projections using the FIJI
313 software (NIH Image). Images were prepared using Imaris, FIJI and Adobe Photoshop CS5.
314 Final figures were constructed using Adobe Illustrator CS5.1.
315
316 **Laser dendrotomies**
317 Micropoint, pulsed nitrogen laser, or the tunable Chameleon Ultra Ti-Sapphire laser system
318 (two-photon), were used to sever the primary dendrite of the PVD. The Micropoint system
319 was used on the Nikon eclipse Ti inverted microscope with Yokogawa CSU-X1 spinning
320 disk. In order to transect neurons, we used 405 beamsplitter and 365nm dye cell and either
321 IQ or Metamorph software. We used highest levels with the attenuator plate (all the way in),
322 while the software controlled attenuator was adjusted between 80-90% when using IQ, and
323 30-50% when using Metamorph. Roughly 15 pulses at 10 Hz were administered for each cut
324 in IQ and Metamorph. For all worms the primary dendrite was injured anterior to cell body.
325 Animals were imaged and a z-stack was collected immediately after cut to confirm that the
326 injury was successful.
327 The two-photon system was used on the Zeiss LSM 510 META microscope. The
328 laser produces 200fs short pulses at 113MHz repetition rate and energy of 5nJ. In order to
329 cut neurons we used 820 nm wavelength and 20-30% laser power using the Zen software.
330 Worms were imaged immediately after cut to confirm that the injury was successful, and z-
331 stacks were taken using the spinning disk confocal system or the LSM 510 META as
332 described for live imaging of worms. After surgery, animals were recovered on NGM agar
333 plates seeded with OP50 in a drop of M9 and imaged again later, or time-lapse movies were
334 immediately acquired.

335 Regeneration was defined as continuation of the fluorescent signal between the distal and
336 proximal ends or using Kaede photoconversion (**Figure 6-figure supplement 1**; see below).
337 Significant differences between ages and genotypes were determined using *Fisher's exact*
338 *test.*
339
340 **Kaede photoconversion**
341 In order to verify that dendrites fuse as response to injury we used the photoconvertible
342 protein Kaede driven by a PVD specific promoter *ser-2prom3*. Irreversible photoconversion
343 of the green Kaede to red Kaede was achieved using Mosaic system on the Nikon eclipse Ti
344 inverted microscope with Yokogawa CSU-X1 spinning disk, at 405 nm, 20-50 ms exposure
345 time with 10-20 repeats across the region of interest, which was always the cell body, using
346 either IQ or Metamorph software.
347
348 **Morphological quantitation of the PVD**
349 Branch count and disorganization of menorahs was counted in the 100 µm around cell body
350 (unless otherwise stated), as previously described [23]. Lack of self-avoidance between
351 adjacent menorahs was determined in the same region as previously described [40]. Z-stack
352 maximum intensity projections of time-lapse movies were analyzed manually, using FIJI
353 software. Factorial analysis of variance (ANOVA) and *t-tests* were performed to compare
354 between genotypes and ages.
355
356 **Harsh touch assay**
357 Harsh touch assay was performed as previously described [23,41] and the experimenter was
358 blind to the genotype. The experiments were done in light touch mutant background (*mec-*

359 *4(e1611)*) [54]. *mec-3(e1338)* worms were used as negative control [41]. Significant differences
360 between the ages were determined by the $\chi 2$ test.
361
362 **Life-span assay**
363 Lifespan assays were carried out at 20°C as previously described [55]. A population of worms
364 was synchronized using hypochlorite and NaOH solution and ~100 animals at the L4
365 "Christmas tree" stage were placed on NGM plates containing 49.5 μM 5-Fluoro-2′-
366 deoxyuridine (FUDR, Sigma, F0503) seeded with OP50 *E. coli*, at a density of 20 worms per
367 6 cm plate. Adult day 1 was designated as the day after the L4 larval stage that served as
368 time 0. Animals were scored as dead or alive every 2-3 days until all animals died. An
369 animal was scored dead when it did not move or react at all to prodding with a platinum wire.
370 Animals that crawled off of the plate, were trapped in fungal infection, "exploded" (i.e.,
371 showed extruded tissue from the vulva), or showed internal hatching ("bagging"), were
372 excluded. If plates were contaminated, animals were transferred to fresh plates, using
373 platinum wire. Statistical significance was determined using the Log-Rank (Mantel-Cox)
374 test.
375
376 **RNA Isolation, Reverse Transcription, and Quantitative Real-Time PCR.**
377 Total RNA from Wild-type worms and des-2p::AFF-1 transgenic worms was isolated using
378 the RNeasy Micro kit following the manufacturer's protocol (Qiagen). RNA was used for
379 cDNA synthesis using the qScript cDNA Synthesis Kit (Quanta BioSciences) with random
380 primers. Real-time PCR was performed using AFF-1 and Fast SYBR® Green Master Mix
381 (Applied Biosystems). The PCR amplification conditions were as follows: 40 cycles of 95 °C
382 for 20 s and 60 °C for 20 s. Each PCR was run in triplicate. Data analysis and quantification
383 were performed using StepOne software V2.2 supplied by Applied Biosystems. To account

384 for the variability in the initial concentration of the RNA, results were normalized to the

385 ACT-1 housekeeping gene.

386

387 **Statistical analysis**

388 Statistical analysis was performed using the GraphPad online tool:

389 http://www.graphpad.com/quickcalcs/ for *t-tests, Fisher's exact test*s and χ^2 tests. Analysis of

390 variance (ANOVA) that was performed when more than two groups were compared and Log-

391 Rank survival test, using SPSS. *Freeman-Halton* extension of the *Fisher's exact test* (for 2x4

392 contingency table) was performed using the Vassarstats.net online tool, to compare between

393 the distributions of response to injury between different genotypes and ages.

394

395 **References**

396 1 Yankner, B. A., Lu, T. & Loerch, P. in *Annual Review of Pathology-Mechanisms of Disease* Vol. 3
397 *Annual Review of Pathology-Mechanisms of Disease* 41-66 (Annual Reviews, 2008).
398 2 Kenyon, C. J. The genetics of ageing. *Nature* **464**, 504-512, doi:10.1038/nature08980 (2010).
399 3 Hammarlund, M. & Jin, Y. Axon regeneration in C. elegans. *Current Opinion in Neurobiology* **27**,
400 199-207, doi:10.1016/j.conb.2014.04.001 (2014).
401 4 Ghosh-Roy, A. & Chisholm, A. D. Caenorhabditis elegans: A new model organism for studies of axon
402 regeneration. *Developmental Dynamics* **239**, 1460-1464, doi:10.1002/dvdy.22253 (2010).
403 5 Kenyon, C., Chang, J., Gensch, E., Rudner, A. & Tabtiang, R. A C-elegans mutant the lives twice as
404 long as wild- type *Nature* **366**, 461-464, doi:10.1038/366461a0 (1993).
405 6 Lin, K., Hsin, H., Libina, N. & Kenyon, C. Regulation of the Caenorhabditis elegans longevity protein
406 DAF-16 by insulin/IGF-1 and germline signaling. *Nature Genetics* **28**, 139-145, doi:10.1038/88850
407 (2001).
408 7 Murphy, C. T., McCarroll, S. A., Bargmann, C. I., Fraser, A., Kamath, R. S., Ahringer, J., Li, H. &
409 Kenyon, C. Genes that act downstream of DAF-16 to influence the lifespan of Caenorhabditis elegans.
410 *Nature* **424**, 277-284, doi:10.1038/nature01789 (2003).
411 8 Tank, E. M. H., Rodgers, K. E. & Kenyon, C. Spontaneous age-related neurite branching in
412 Caenorhabditis elegans. *J. Neurosci.* **31**, 9279-9288, doi:10.1523/jneurosci.6606-10.2011 (2011).
413 9 Toth, M. L., Melentijevic, I., Shah, L., Bhatia, A., Lu, K., Talwar, A., Naji, H., Ibanez-Ventoso, C.,
414 Ghose, P., Jevince, A., Xue, J., Herndon, L. A., Bhanot, G., Rongo, C., Hall, D. H. & Driscoll, M.
415 Neurite sprouting and synapse deterioration in the aging Caenorhabditis elegans nervous system. *J.*
416 *Neurosci.* **32**, 8778-8790, doi:10.1523/jneurosci.1494-11.2012 (2012).
417 10 Pan, C.-L., Peng, C.-Y., Chen, C.-H. & McIntire, S. Genetic analysis of age-dependent defects of the
418 Caenorhabditis elegans touch receptor neurons. *Proc. Natl. Acad. Sci. U.S.A.* **108**, 9274-9279,
419 doi:10.1073/pnas.1011711108 (2011).
420 11 Byrne, A. B., Walradt, T., Gardner, K. E., Hubbert, A., Reinke, V. & Hammarlund, M. Insulin/IGF1
421 signaling inhibits age-dependent axon regeneration. *Neuron* **81**, 561-573,
422 doi:10.1016/j.neuron.2013.11.019 (2014).
423 12 Neumann, B., Coakley, S., Giordano-Santini, R., Linton, C., Lee, E. S., Nakagawa, A., Xue, D. &
424 Hilliard, M. A. EFF-1-mediated regenerative axonal fusion requires components of the apoptotic
425 pathway. *Nature* **517**, 219-U259, doi:10.1038/nature14102 (2015).

13 Neumann, B., Nguyen, K. C. Q., Hall, D. H., Ben-Yakar, A. & Hilliard, M. A. Axonal Regeneration Proceeds Through Specific Axonal Fusion in Transected C. elegans Neurons. *Developmental Dynamics* **240**, 1365-1372, doi:10.1002/dvdy.22606 (2011).

14 Hoy, R. R., Bittner, G. D. & Kennedy, D. Regeneration in Crustacean motoneurons - evidence for axonal fusion *Science* **156**, 251-&, doi:10.1126/science.156.3772.251 (1967).

15 Ghosh-Roy, A., Wu, Z. L., Goncharov, A., Jin, Y. S. & Chisholm, A. D. Calcium and cyclic AMP promote axonal regeneration in Caenorhabditis elegans and require DLK-1 kinase. *J. Neurosci.* **30**, 3175-3183, doi:10.1523/jneurosci.5464-09.2010 (2010).

16 Paltsyn, A., Komissarova, S., Dubrovin, I. & Kubatiev, A. Increased cell fusion in cerebral cortex may contribute to poststroke regeneration. *Stroke research and treatment* **2013**, 869327-869327, doi:10.1155/2013/869327 (2013).

17 Alvarez-Dolado, M., Pardal, R., Garcia-Verdugo, J. M., Fike, J. R., Lee, H. O., Pfeffer, K., Lois, C., Morrison, S. J. & Alvarez-Buylla, A. Fusion of bone-marrow-derived cells with Purkinje neurons, cardiomyocytes and hepatocytes. *Nature* **425**, 968-973, doi:http://www.nature.com/nature/journal/v425/n6961/suppinfo/nature02069_S1.html (2003).

18 Johansson, C. B., Youssef, S., Koleckar, K., Holbrook, C., Doyonnas, R., Corbel, S. Y., Steinman, L., Rossi, F. M. V. & Blau, H. M. Extensive fusion of haematopoietic cells with Purkinje neurons in response to chronic inflammation. *Nature Cell Biology* **10**, 575-583, doi:10.1038/ncb1720 (2008).

19 Mohler, W. A., Shemer, G., del Campo, J. J., Valansi, C., Opoku-Serebuoh, E., Scranton, V., Assaf, N., White, J. G. & Podbilewicz, B. The type I membrane protein EFF-1 is essential for developmental cell fusion. *Developmental Cell* **2**, 355-362, doi:10.1016/s1534-5807(02)00129-6 (2002).

20 Podbilewicz, B., Leikina, E., Sapir, A., Valansi, C., Suissa, M., Shemer, G. & Chernomordik, L. V. The C-elegans developmental fusogen EFF-1 mediates homotypic fusion in heterologous cells and in vivo. *Developmental Cell* **11**, 471-481, doi:10.1016/j.devcel.2006.09.004 (2006).

21 Shemer, G., Suissa, M., Kolotuev, I., Nguyen, K. C. Q., Hall, D. H. & Podbilewicz, B. EFF-1 Is Sufficient to Initiate and Execute Tissue-Specific Cell Fusion in C. elegans. *Current Biology* **14**, 1587-1591, doi:10.1016/j.cub.2004.07.059 (2004).

22 Tsalik, E. L., Niacaris, T., Wenick, A. S., Pau, K., Avery, L. & Hobert, O. LIM homeobox gene-dependent expression of biogenic amine receptors in restricted regions of the C-elegans nervous system. *Developmental Biology* **263**, 81-102, doi:10.1016/s0012-1606(03)00447-0 (2003).

23 Oren-Suissa, M., Hall, D. H., Treinin, M., Shemer, G. & Podbilewicz, B. The fusogen EFF-1 controls sculpting of mechanosensory dendrites. *Science* **328**, 1285-1288, doi:10.1126/science.1189095 (2010).

24 Smith, C. J., Watson, J. D., Spencer, W. C., O'Brien, T., Cha, B., Albeg, A., Treinin, M. & Miller, D. M., III. Time-lapse imaging and cell-specific expression profiling reveal dynamic branching and molecular determinants of a multi-dendritic nociceptor in C. elegans. *Dev. Biol.* **345**, 18-33, doi:10.1016/j.ydbio.2010.05.502 (2010).

25 Chatzigeorgiou, M., Yoo, S., Watson, J. D., Lee, W. H., Spencer, W. C., Kindt, K. S., Hwang, S. W., Miller, D. M., Treinin, M., Driscoll, M. & Schafer, W. R. Specific roles for DEG/ENaC and TRP channels in touch and thermosensation in C. elegans nociceptors. *Nat. Neurosci.* **13**, 861-U106, doi:10.1038/nn.2581 (2010).

26 Salzberg, Y., Diaz-Balzac, C. A., Ramirez-Suarez, N. J., Attreed, M., Tecle, E., Desbois, M., Kaprielian, Z. & Buelow, H. E. Skin-derived cues control arborization of sensory dendrites in Caenorhabditis elegans. *Cell* **155**, 308-320, doi:10.1016/j.cell.2013.08.058 (2013).

27 Dong, X., Liu, O. W., Howell, A. S. & Shen, K. An extracellular adhesion molecule complex patterns dendritic branching and morphogenesis. *Cell* **155**, 296-307, doi:10.1016/j.cell.2013.08.059 (2013).

28 Dong, X., Shen, K. & Bülow, H. E. Intrinsic and Extrinsic Mechanisms of Dendritic Morphogenesis. *Annual Review of Physiology* **77**, null, doi:doi:10.1146/annurev-physiol-021014-071746 (2015).

29 Liu, O. W. & Shen, K. The transmembrane LRR protein DMA-1 promotes dendrite branching and growth in C. elegans. *Nat. Neurosci.* **15**, 57-U74, doi:10.1038/nn.2978 (2012).

30 Maniar, T. A., Kaplan, M., Wang, G. J., Shen, K., Wei, L., Shaw, J. E., Koushika, S. P. & Bargmann, C. I. UNC-33 (CRMP) and ankyrin organize microtubules and localize kinesin to polarize axon-dendrite sorting. *Nat. Neurosci.* **15**, 48-U66, doi:10.1038/nn.2970 (2012).

31 Cohen, E., Chatzigeorgiou, M., Husson, S. J., Steuer-Costa, W., Gottschalk, A., Schafer, W. R. & Treinin, M. Caenorhabditis elegans nicotinic acetylcholine receptors are required for nociception. *Molecular and Cellular Neuroscience* **59**, 85-96, doi:10.1016/j.mcn.2014.02.001 (2014).

32 Husson, S. J., Costa, W. S., Wabnig, S., Stirman, J. N., Watson, J. D., Spencer, W. C., Akerboom, J., Looger, L. L., Treinin, M., Miller, D. M., III, Lu, H. & Gottschalk, A. Optogenetic Analysis of a Nociceptor Neuron and Network Reveals Ion Channels Acting Downstream of Primary Sensors. *Current Biology* **22**, 743-752, doi:10.1016/j.cub.2012.02.066 (2012).

33 Wei, X., Howell, A. S., Dong, X., Taylor, C. A., Cooper, R. C., Zhang, J., Zou, W., Sherwood, D. R. & Shen, K. The unfolded protein response is required for dendrite morphogenesis. *eLife* **4**, e06963, doi:10.7554/eLife.06963 (2015).

34 Sapir, A., Choi, J., Leikina, E., Avinoam, O., Valansi, C., Chernomordik, L. V., Newman, A. P. & Podbilewicz, B. AFF-1, a FOS-1-regulated fusogen, mediates fusion of the anchor cell in C-elegans. *Dev. Cell* **12**, 683-698, doi:10.1016/j.devcel.2007.03.003 (2007).

35 Oren-Suissa, M., Gattegno, T., Kravtsov, V. & Podbilewicz, B. Extrinsic repair of injured dendrites as a paradigm for regeneration by fusion. *Submitted to eLife* (2016).

36 Procko, C., Lu, Y. & Shaham, S. Glia delimit shape changes of sensory neuron receptive endings in C. elegans. *Development* **138**, 1371-1381, doi:10.1242/dev.058305 (2011).

37 Stone, C. E., Hall, D. H. & Sundaram, M. V. Lipocalin signaling controls unicellular tube development in the Caenorhabditis elegans excretory system. *Developmental Biology* **329**, 201-211, doi:10.1016/j.ydbio.2009.02.030 (2009).

38 Rasmussen, J. P., English, K., Tenlen, J. R. & Priess, J. R. Notch signaling and morphogenesis of single-cell tubes in the C-elegans digestive tract. *Developmental Cell* **14**, 559-569, doi:10.1016/j.devcel.2008.01.019 (2008).

39 Lenard, A., Daetwyler, S., Betz, C., Ellertsdottir, E., Belting, H.-G., Huisken, J. & Affolter, M. Endothelial cell self-fusion during vascular pruning. *PLoS biology* **13**, e1002126-e1002126, doi:10.1371/journal.pbio.1002126 (2015).

40 Smith, C. J., Watson, J. D., VanHovene, M. K., Colon-Ramos, D. A. & Miller, D. M., III. Netrin (UNC-6) mediates dendritic self-avoidance. *Nat. Neurosci.* **15**, 731-737, doi:10.1038/nn.3065 (2012).

41 Way, J. C. & Chalfie, M. The mec-3 gene of Caenorhabditis-elegans requires its own product for maintained expression and is expressed in 3 neuronal cell-types *Genes Dev.* **3**, 1823-1833, doi:10.1101/gad.3.12a.1823 (1989).

42 Verdu, E., Ceballos, D., Vilches, J. J. & Navarro, X. Influence of aging on peripheral nerve function and regeneration. *J. Periph. Nerv. Syst.* **5**, 191-208, doi:10.1046/j.1529-8027.2000.00026.x (2000).

43 Zou, Y., Chiu, H., Zinovyeva, A., Ambros, V., Chuang, C.-F. & Chang, C. Developmental decline in neuronal regeneration by the progressive change of two intrinsic timers. *Science* **340**, 372-376, doi:10.1126/science.1231321 (2013).

44 Jan, Y. N. & Jan, L. Y. Branching out: mechanisms of dendritic arborization. *Nat. Rev. Neurosci.* **11**, 316-328, doi:10.1038/nrn2836 (2010).

45 Koleske, A. J. Molecular mechanisms of dendrite stability. *Nat. Rev. Neurosci.* **14**, 536-550, doi:10.1038/nrn3486 (2013).

46 Buell, S. J. & Coleman, P. D. Dendritic growth in the aged human-brain and failure of growth in senile dementia *Science* **206**, 854-856, doi:10.1126/science.493989 (1979).

47 Hammarlund, M., Nix, P., Hauth, L., Jorgensen, E. M. & Bastiani, M. Axon regeneration requires a conserved MAP kinase pathway. *Science* **323**, 802-806, doi:10.1126/science.1165527 (2009).

48 Gabel, C. V., Antonie, F., Chuang, C.-F., Samuel, A. D. T. & Chang, C. Distinct cellular and molecular mechanisms mediate initial axon development and adult-stage axon regeneration in C. elegans. *Development* **135**, 1129-1136, doi:10.1242/dev.013995 (2008).

49 Pestronk, A., Drachman, D. B. & Griffin, J. W. Effects of aging on nerve sprouting and regeneration *Exp. Neurol.* **70**, 65-82, doi:10.1016/0014-4886(80)90006-0 (1980).

50 Brenner, S. Genetics of Caenorhabditis-elegans *Genetics* **77**, 71-94 (1974).

51 Yip, Z. C. & Heiman, M. G. Duplication of a Single Neuron in C. elegans Reveals a Pathway for Dendrite Tiling by Mutual Repulsion. *Cell reports*, doi:10.1016/j.celrep.2016.05.003 (2016).

52 Sarov, M., Schneider, S., Pozniakovski, A., Roguev, A., Ernst, S., Zhang, Y., Hyman, A. A. & Stewart, A. F. A recombineering pipeline for functional genomics applied to Caenorhabditis elegans. *Nat Methods* **3**, 839-844, doi:10.1038/nmeth933 (2006).

53 del Campo, J. J., Opoku-Serebuoh, E., Isaacson, A. B., Scranton, V. L., Tucker, M., Han, M. & Mohler, W. A. Fusogenic activity of EFF-1 is regulated via dynamic localization in fusing somatic cells of C. elegans. *Curr Biol* **15**, 413-423 (2005).

54 Chalfie, M. & Sulston, J. Developmental genetics of the mechanosensory neurons of Caenorhabditis-elegans *Dev. Biol.* **82**, 358-370, doi:10.1016/0012-1606(81)90459-0 (1981).

55 Apfeld, J. & Kenyon, C. Cell nonautonomy of C-elegans daf-2 function in the regulation of diapause and life span. *Cell* **95**, 199-210, doi:10.1016/s0092-8674(00)81751-1 (1998).

Figures

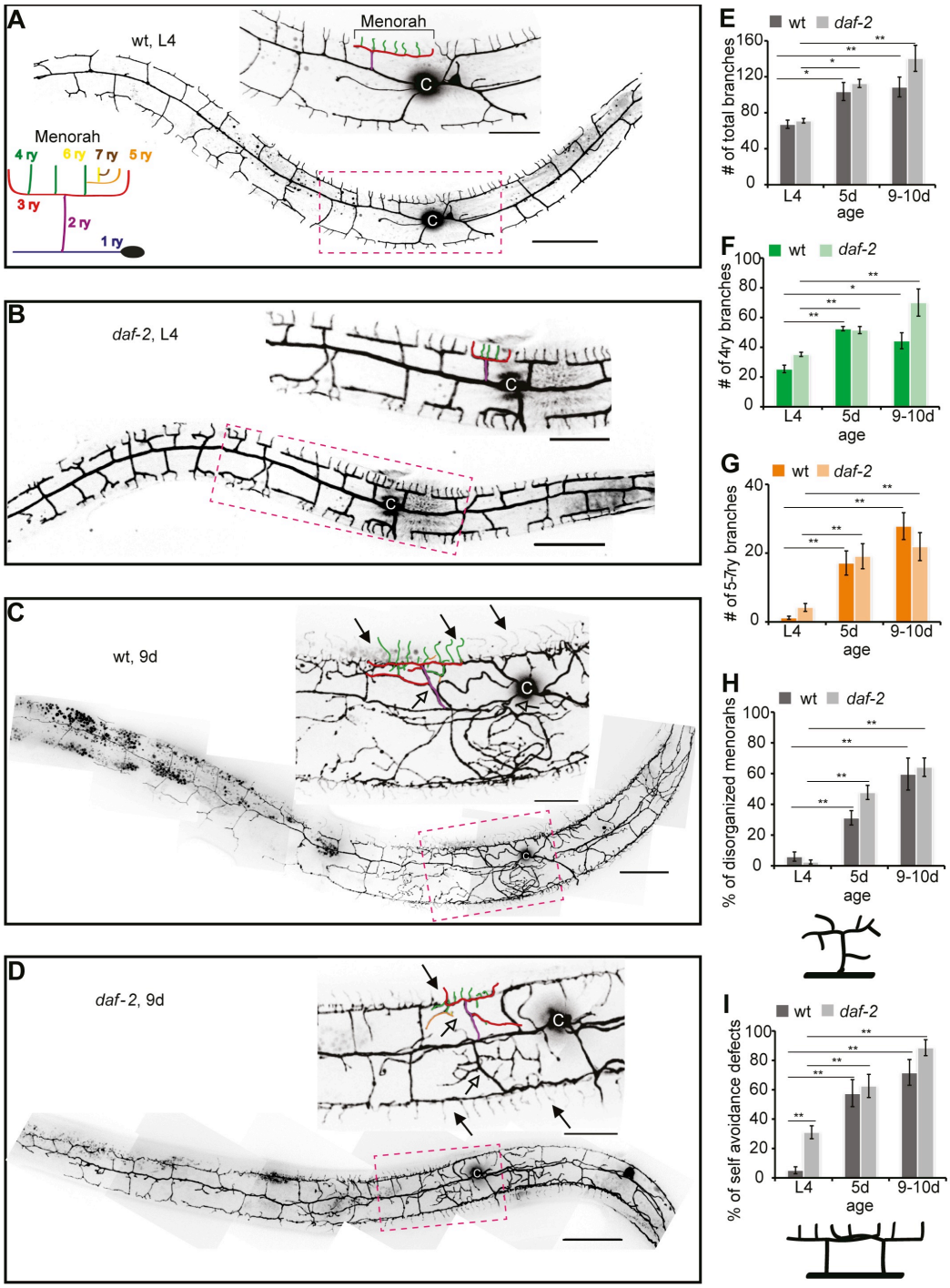

Figure 1.
PVD's dendritic alterations during aging

(A-D) PVD in wild-type (wt; **A** and **C**) and *daf-2* mutants (**B** and **D**) at L4 stage and 9 days of adulthood (9d). Upper panels, magnified boxed areas with "menorah" colored according to the scheme (**A).** c, cell body. Scale bars, 50 µm and 20 µm in magnified images. Anterior is left and ventral is down in all the figures. Filled arrows, self-avoidance defects. Empty arrows, disorganized menorahs. **(E-I)** Quantitation of phenotypes shown in images. Percentages are for 100 µm of length around cell body. Error bars, ± s.e.m. *p* values from *t* tests: *$p<0.01$, **$p<0.001$. Number of animals analyzed: *daf-2* n ≥ 8 and wild-types n ≥ 5.

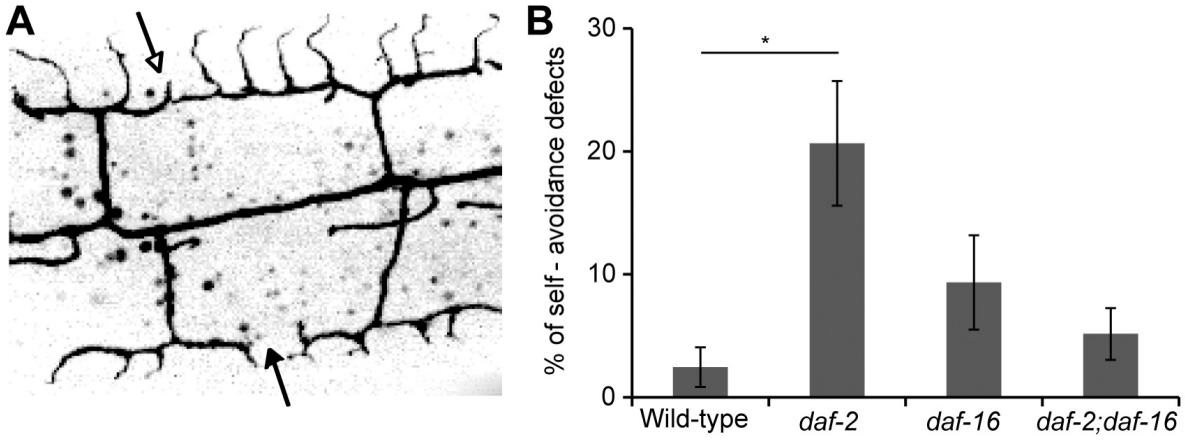

555

556

557 **Figure 2.**

558 **DAF-2-DAF-16 control menorah self-avoidance at L4 stage**

559 **(A)** Image showing four wild-type menorahs labeled with GFP, two of them do not overlap
560 (filled arrow) and two show defective self-avoidance (empty arrow).

561 **(B)** Percentage of defects in self-avoidance in 100 µm of length around PVD cell body at L4
562 stage in different genotypes, n ≥ 7. Defective self-avoidance increased in *daf-2* mutants in a
563 *daf-16*-dependent manner. Error bars are ± s.e.m. *p* value from *t* test: * $p<0.05$.

564

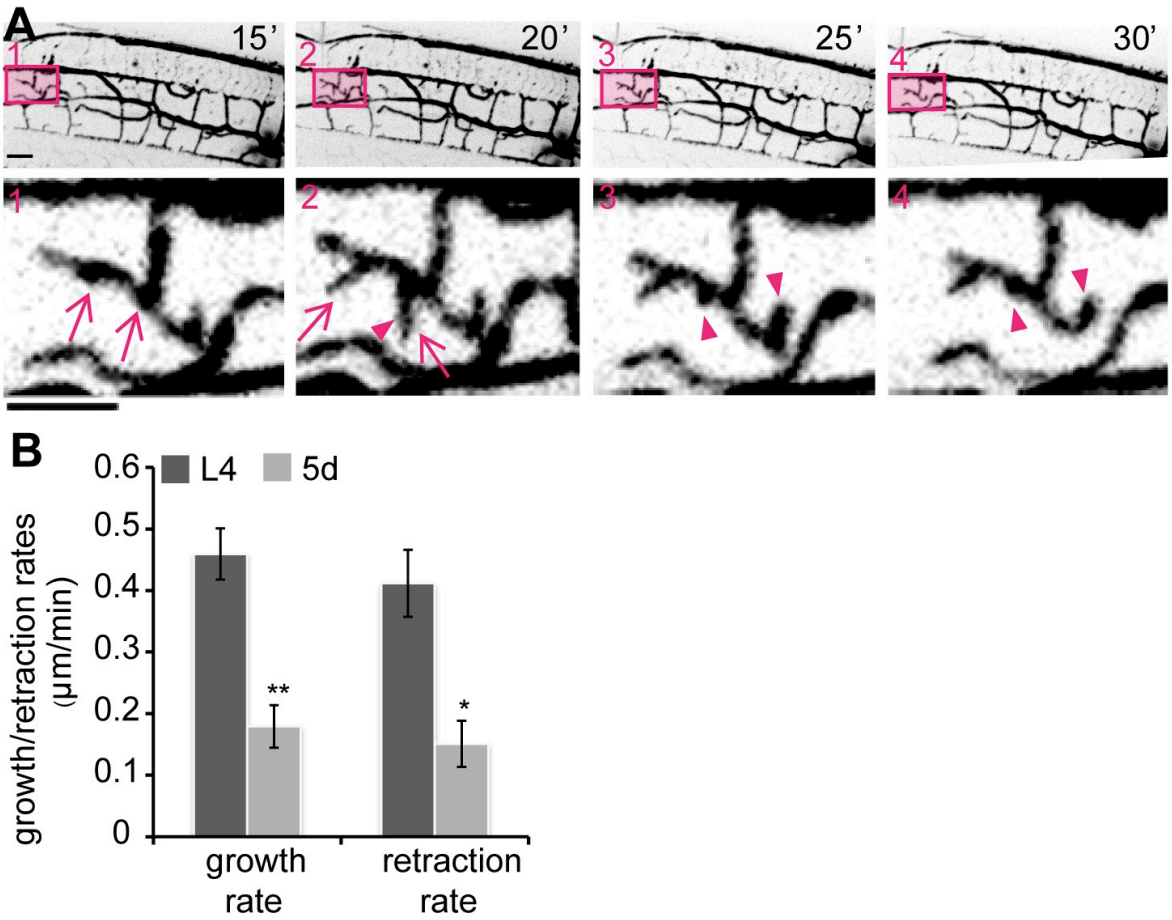

Figure 3.

Adults show a reduction in dendritic plasticity

(A) Time-lapse confocal projections of 5 days of adulthood (5d) wild-type animal. Boxed areas are enlarged in the lower panel and reveal dynamic growth (arrows) and retraction (arrow heads) of branches. Scale bars, 10 µm.

(B) Growth and retraction rates in µm/minute of branches at L4 stage and 5d as measured from time-lapse movies. Number of branches analyzed ≥ 18 from 4 L4 animals and 2 5d animals. Error bars are ± s.e.m. *p* values from *t* tests: * $p<0.01$, ** $p<0.001$. See also **Movie S1**.

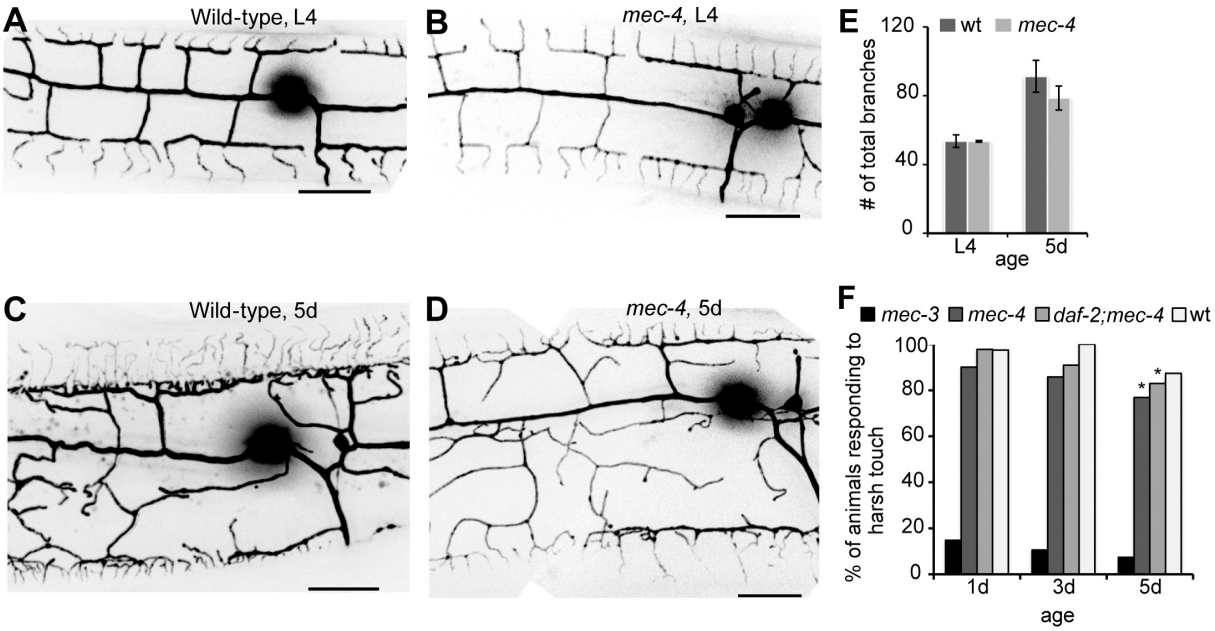

Figure 4.

Decline in response to harsh touch during aging in both wild-type and *daf-2*

(A-D) PVD's cell-body region of wt and light-touch insensitive *mec-4* mutants at the L4 stage and at 5 days of adulthood (5d). Scale bars are 20 µm.

(E) Total number of branches counted in 100 µm of length around cell-body in wt and *mec-4* mutants at L4 and 5d (no significant differences between wt and *mec-4)*. Error bars are ± s.e.m.

(F) Percentage of animals responding to harsh touch by escaping away from the stimulus. At the age of 5d, the response declined in *mec-4* mutants and in *daf-2;mec-4* double mutants. *p* values from $\chi 2$ test as compared between 1d to other ages (3d or 5d) for each genotype: * $p < 0.05$. Number of animals: *mec-3* ≥ 50; *mec-4* ≥ 70; *daf-2;mec-4* ≥ 40; wt ≥ 26.

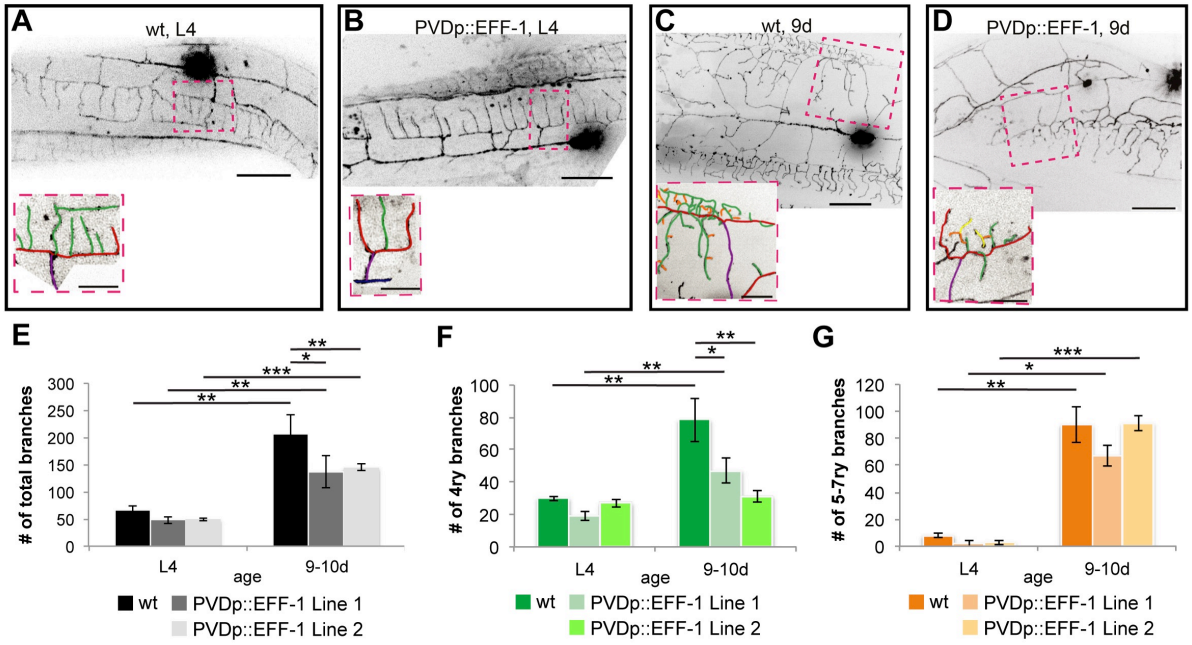

Figure 5.

EFF-1 overexpression in the PVD simplifies "aged" menorahs

(A-D) Inverted fluorescence images of PVD neurons.

(**A** and **C)** Represent wild-type neurons from L4 and 9 days of adulthood (9d).

(**B** and **D)** Represent EFF-1 overexpression under PVD specific promoter (PVDp) at L4 and 9d. In each panel one menorah (boxed) is enlarged and colored (see **Figure 1A**). Scale bars, 20 µm and 10 µm in the enlarged images.

(E-G) Graphs showing number of branches in 100 µm of length around cell body. Error bars, ± s.e.m. *p* values from *t* tests: * $p<0.05$, ** $p<0.001$, *** $p<0.0001$ Number of animals: n ≥ 4. PVDp::EFF-1 line 1 and 2 correspond to worms carrying the extrachromosomal arrays *hyEx392* and *hyEx23,* respectively.

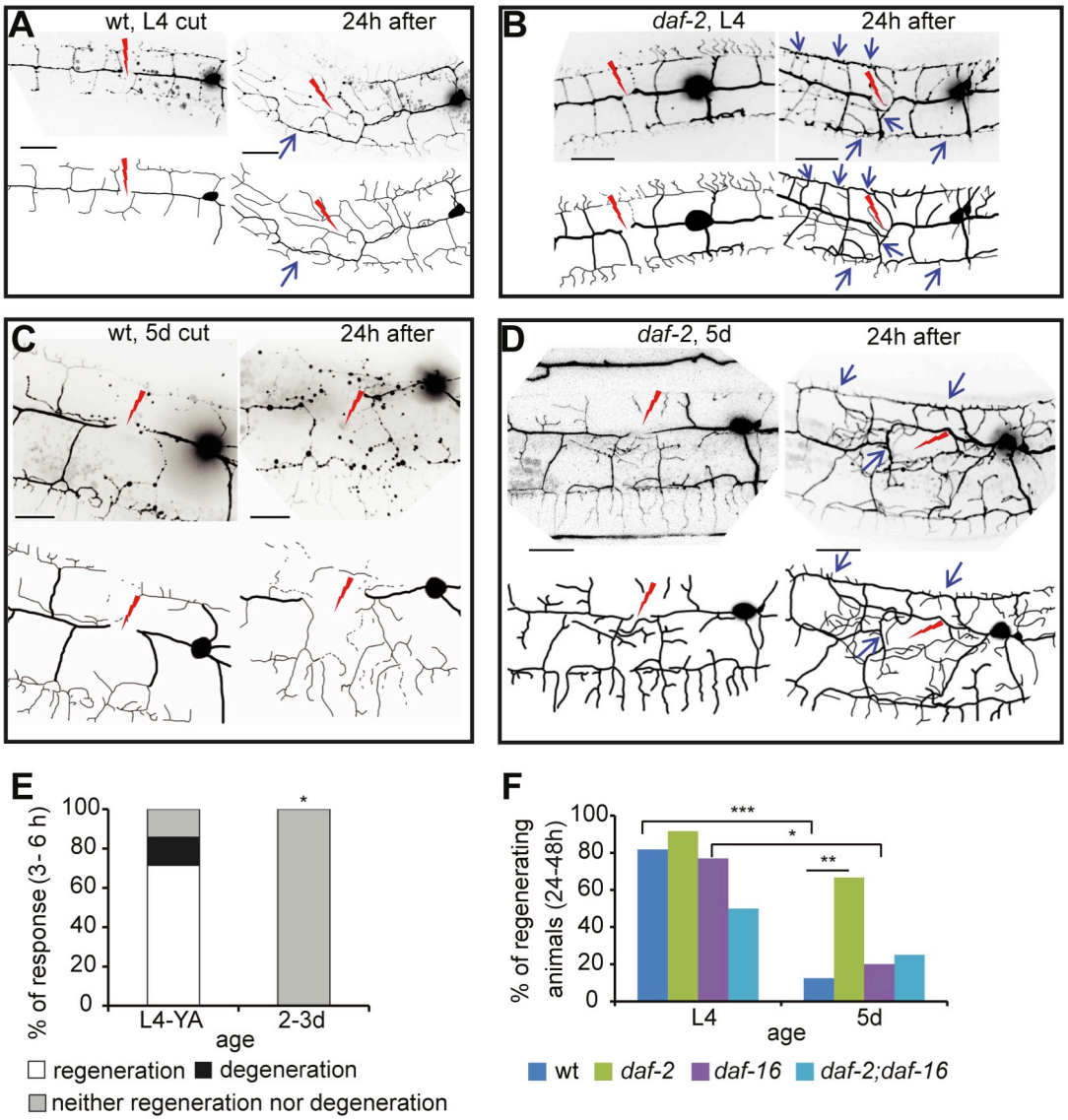

Figure 6.

daf-2*(-) restores regenerative ability of aged animals via *daf-16

(A-D) PVD neurons immediately after cut and 24 h later in wild-type and *daf-2* mutants at L4 and 5 days of adulthood (5d), as indicated. Schematic illustrations below negative images. Red lightings, injury sites. Blue arrows, fusion sites (successful regeneration). Scale bars, 20 µm.

(E) Response to injury of wild-types at L4-young adult (YA) and 2-3d within a short time (3-6 h) after injury. Number of animals: n=7 (L4 –YA) and n=4 (2-3d).

(F) Percentage of successfully regenerating animals within 24-48 h post injury. *p* values from *Fisher's exact tests*: * $p<0.05$, ** $p<0.01$, *** $p<0.001$. Number of animals: n ≥ 8. See also **Figure 6-figure supplement 1** and **Movies S2-S4**.

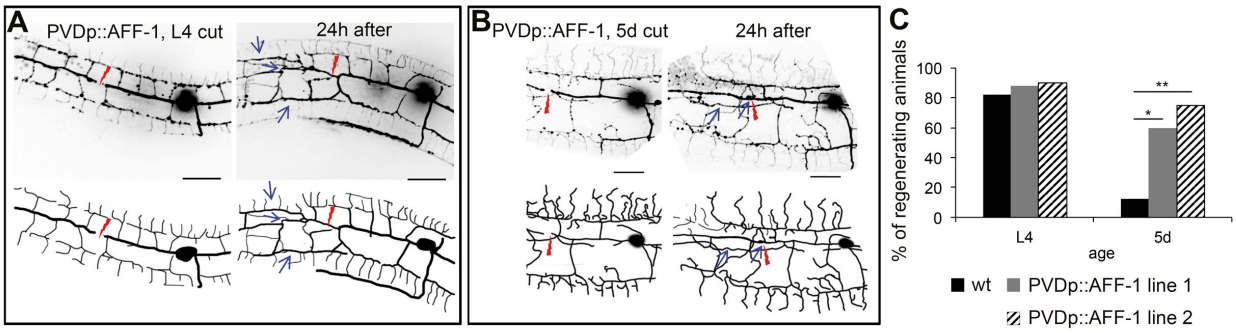

Figure 7.

AFF-1 enhances regeneration by dendrite fusion in 5d-old animals

(A-B) Inverted fluorescence images of PVD neurons immediately after cut and 24 hours (h) later in animals overexpressing AFF-1 in the PVD (PVDp::AFF-1), at L4 and 5 days of adulthood (5d), as indicated on each image (schematic drawings below each image). Red lightning marks the injury site and blue arrows point at fusion sites (menorah-menorah fusion)**.** Scale bars, 20 µm.

(C) Percentage of successfully regenerating animals within 24-48h after injury. *p* value from *Fisher's exact test*: * $p<0.05$; ** $p<0.001$. Number of animals: $n \geq 10$. See also **Figure 7-figure supplement 1** and **Movies S5-S6**. PVDp::AFF-1 line 1 and 2 correspond to worms carrying the extrachromosomal arrays *hyEx390* and *hyEx391,* respectively.

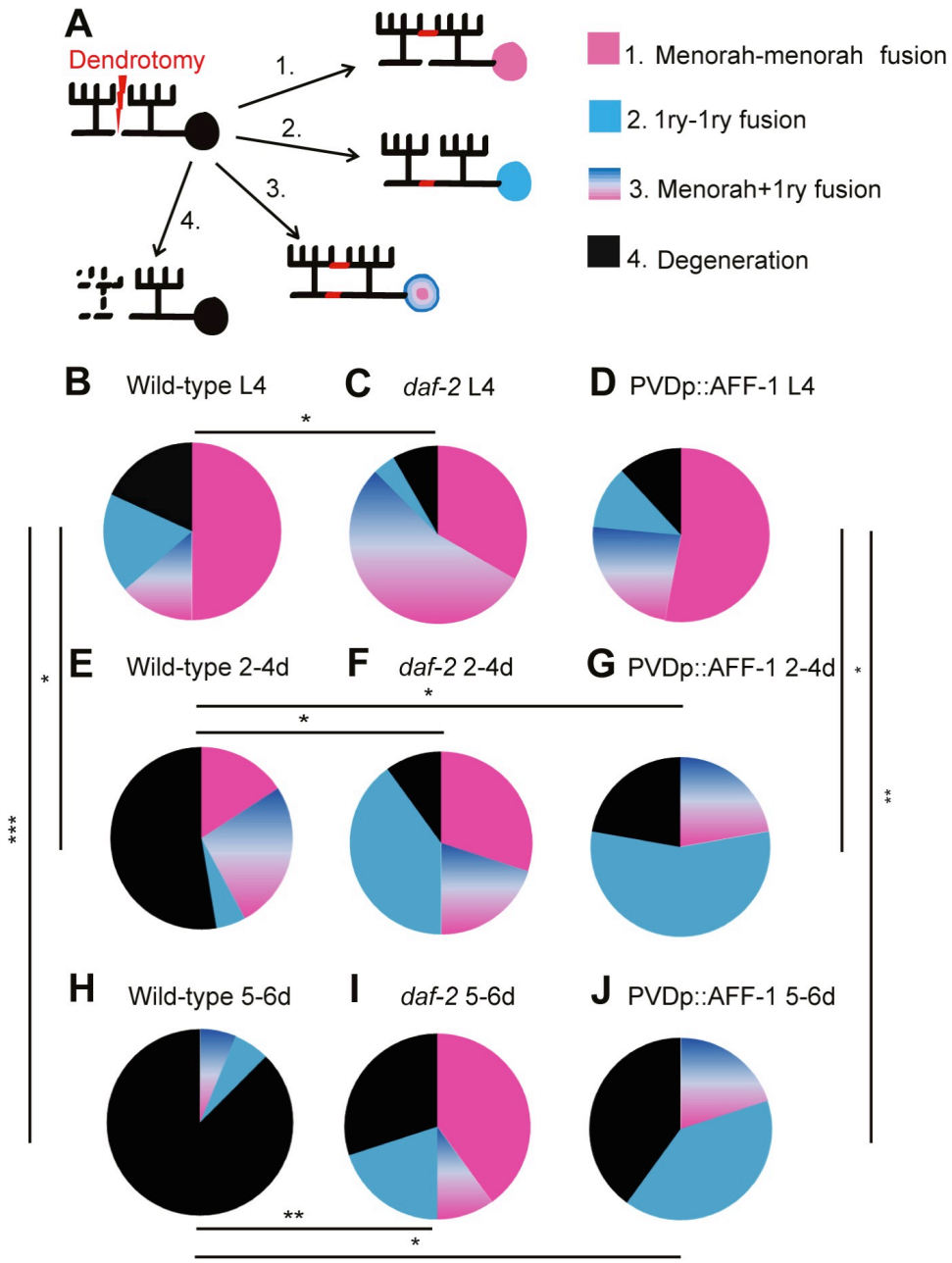

Figure 8.

***daf-2*(-) and AFF-1(+) rejuvenate fusion potential of broken dendrites**

(A) Cartoon representing four possible outcomes of dendrotomy. Dendrite auto-fusion indicates successful regeneration (outcomes 1-3), if fusion does not occur degeneration takes place (outcome 4).

(B-J) Percentages of wild-type worms (wt), *daf-2* mutants and AFF-1 overexpressing animals (PVDp::AFF-1) at different ages, divided into the four different types of response to injury as described in (**A**). Genotype and age are listed above each plot. *p* values from *Fisher's exact tests*: * $p<0.05$, ** $p<0.01$, *** $p<0.001$. Additional significant differences were found between: (**C** and **F**), (**C** and **I**) and between (**B** and **J**) ($p<0.05$). See also **Figure 8-figure supplement 1.**

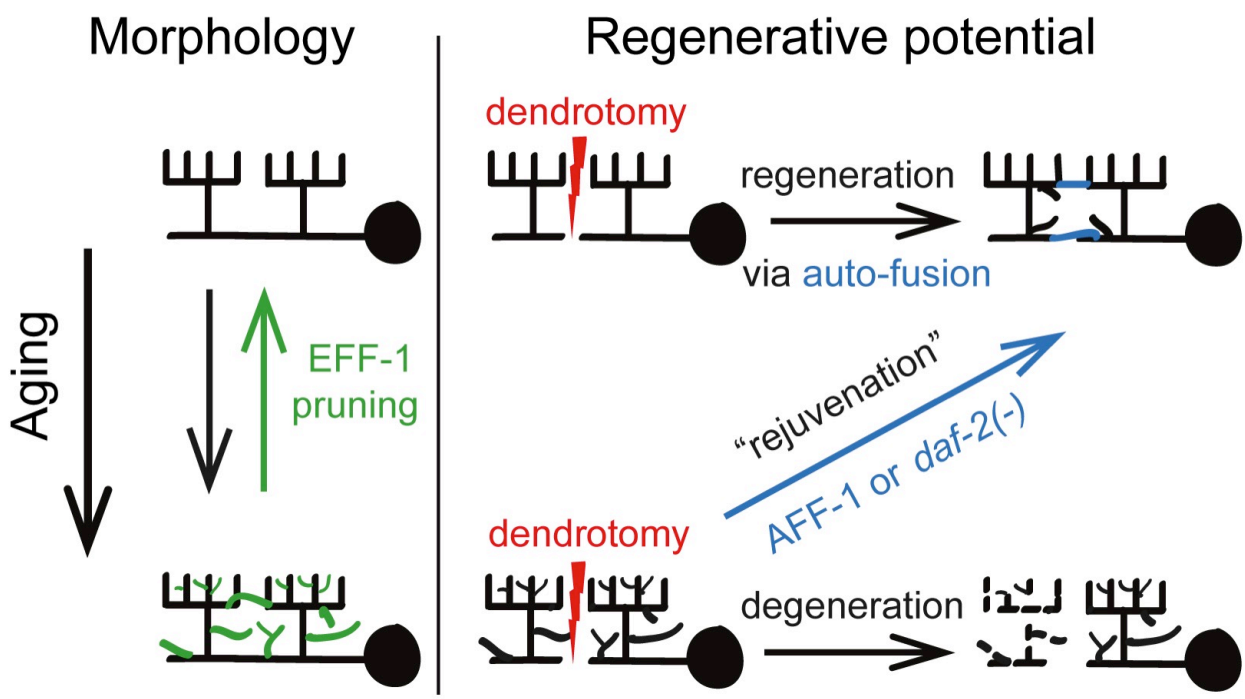

Figure 9.

Model of morphological and regenerative antiaging activities on dendritic arbors

Morphological aging of PVD menorahs is a progressive and dynamic process that results in loss of self-avoidance, disorganization and hyperbranching. When the fusogen EFF-1 is ectopically expressed in the PVD neuron it has an antiaging activity that involves pruning of hyperbranched dendritic trees.

Aged menorahs lose their *regenerative potential* because following laser-induced dendrotomy old neurons usually fail to auto-fuse broken dendrites and undergo degeneration. DAF-2/ IGF-1R negatively regulates the regeneration process. When the fusogen AFF-1 is ectopically expressed in the PVD neuron it has an antiaging activity that promotes auto-fusion of old transected primary dendrites.

Supplementary Figures

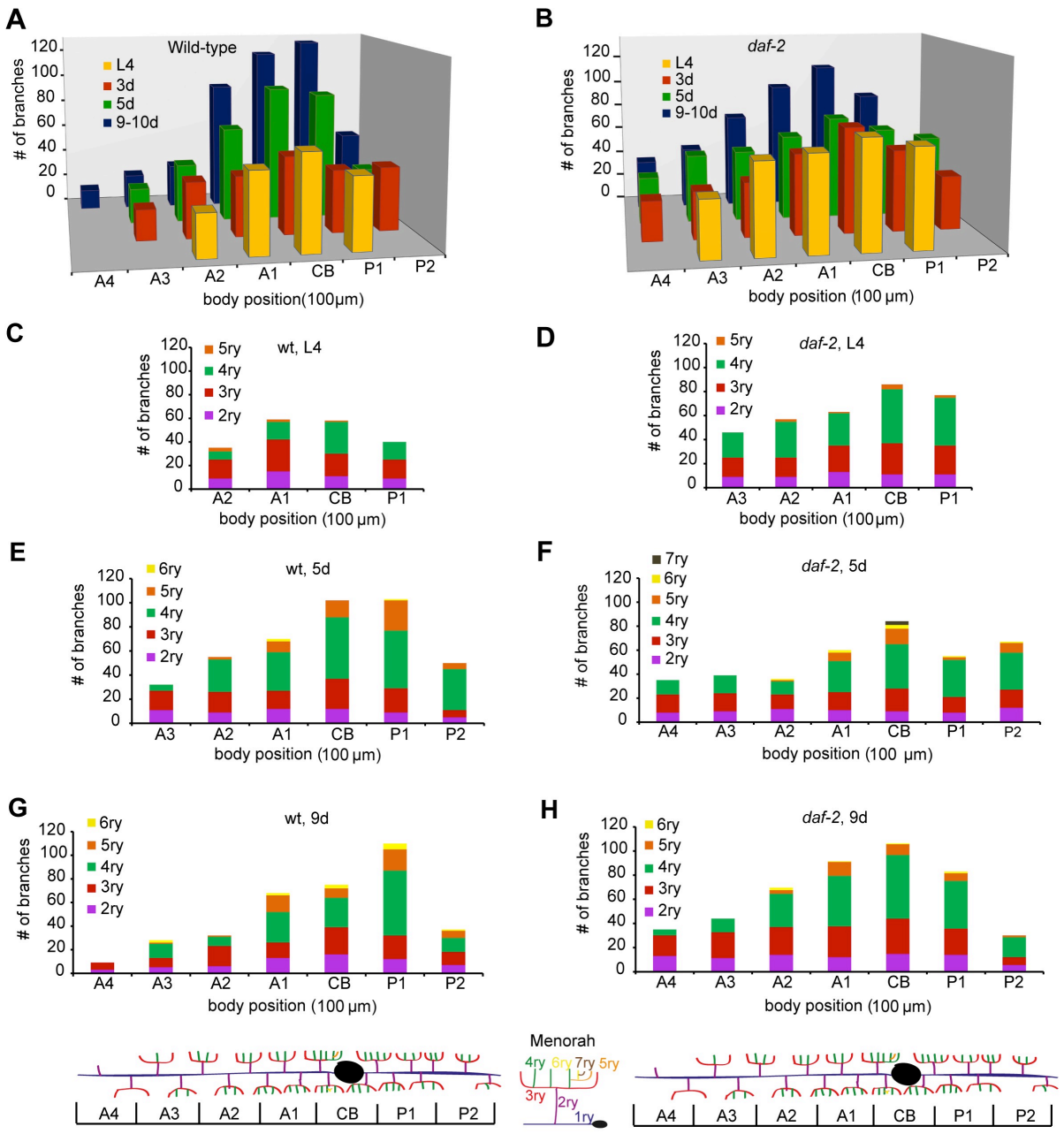

Figure 1-figure supplement 1.

Anterior-posterior branching gradient sharpens as animals age

(A-B) Average number of branches per 100 µm of body length (A4-P2; A, anterior; P, posterior; CB, cell body; d, days of adulthood) in wild-type (wt) and *daf-2* mutants. Gradient sharpening is delayed in *daf-2*. We performed three way analysis of variance (ANOVA) to compare between wt (**A**) and *daf-2* (**B**). The contribution of body position and age to branching were significant (p=0.0001 and p=1.4X10^{-6}, respectively). Age*genotype, body position*genotype, body position*age and genotype alone were significant (p=0.007, p=0.001, p=0.043 and p=0.023, respectively). Number of animals: wt n ≥ 2; *daf-2* n ≥ 3.

(C-H) Each bar is a 100 µm long PVD region. Bars and schematic menorahs on the bottom: 2ry, magenta; 3ry, red; 4ry, green; 5ry, orange; 6ry, yellow; 7ry, brown.

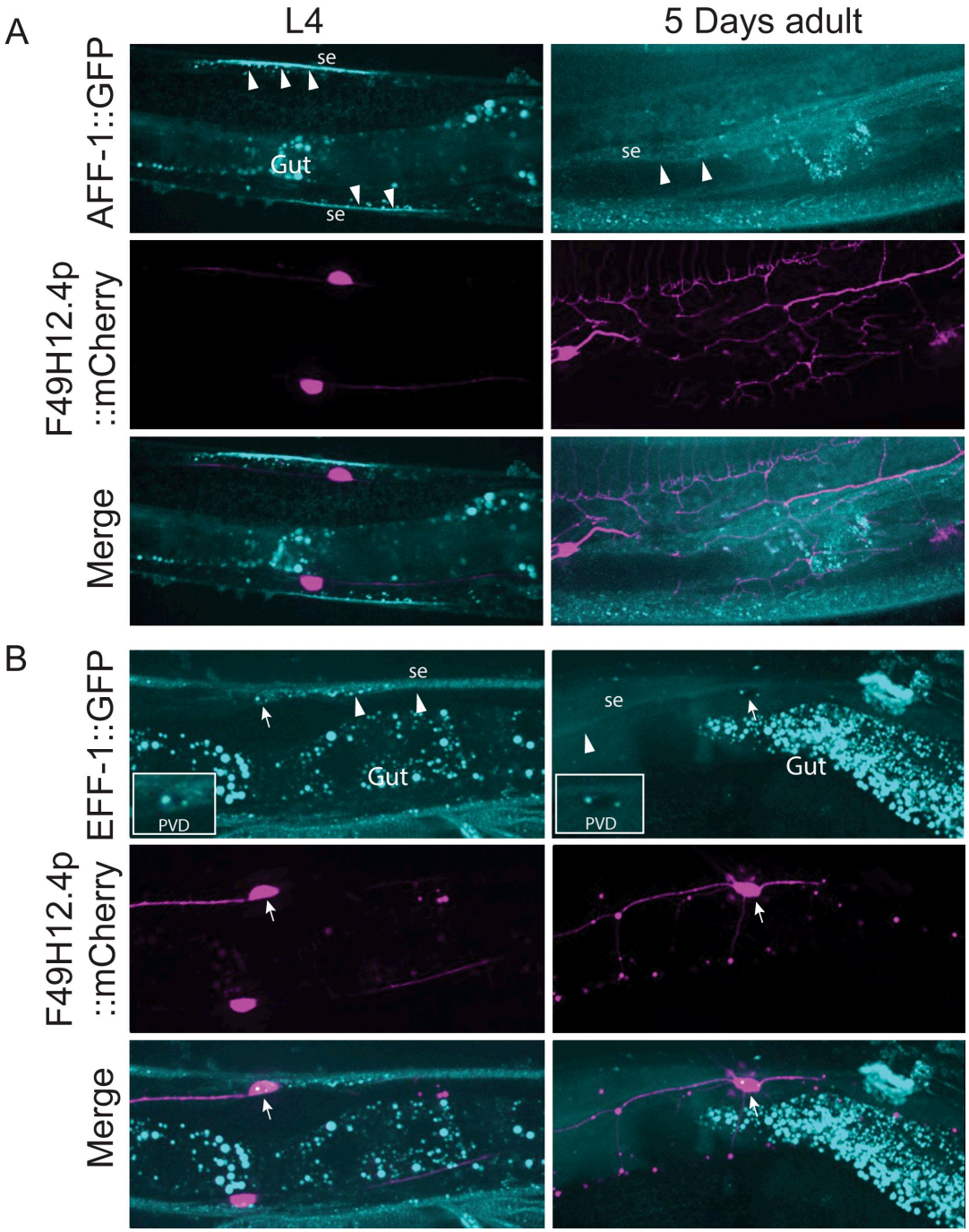

Figure 5-figure supplement 1.

AFF-1 and EFF-1 expression pattern in L4 and aging worms

(A) A 30kb fosmid-based reporter for AFF-1 shows expression in the epithelial seam-cells at the L4 stage (marked with arrowheads), and in 5-day adults. AFF-1 is not expressed at the PVD in any stage. Multiple transgenic lines were analyzed and a similar expression pattern was observed in all.

(B) EFF-1 expression at the L4 stage and 5-days adults was analyzed using an EFF-1::GFP translational chimera: 7.5 kb *eff-1* promoter driving the full-length *eff-1* genomic coding sequence was fused to GFP [53]. EFF-1 is expressed in the seam-cells (arrowheads) and the PVD cell body (arrows and inset) in vesicles. Expression persists after 5 days.

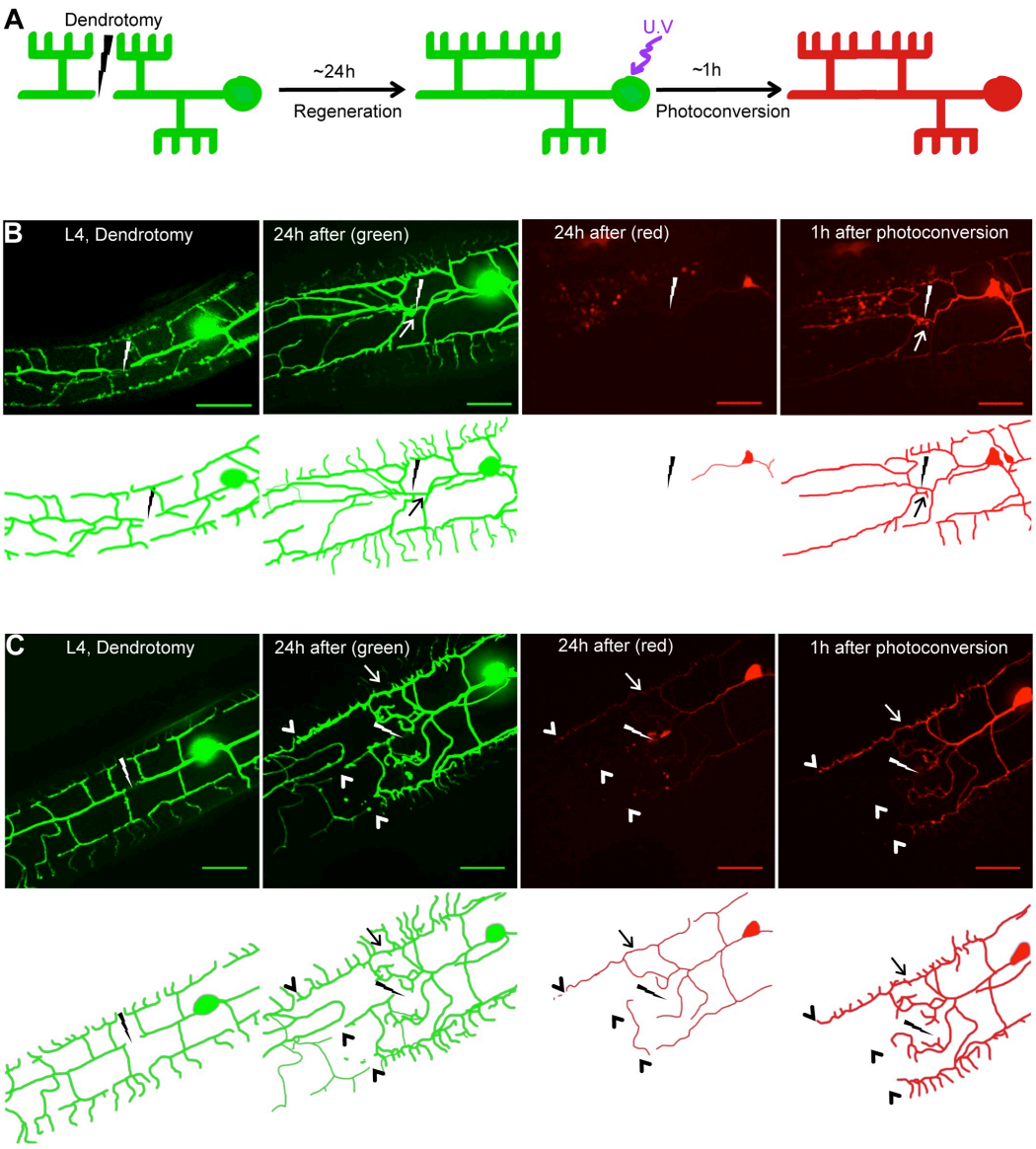

Figure 6-figure supplement 1.

Fusion is a crucial step in regeneration of injured dendrites

(A) Scheme describing the fusion assay using a photoconvertible fluorescent marker Kaede. Primary dendrite is injured using a laser, then the animal is recovered and imaged again after ~24 hours in green and red channels. Green Kaede is photoconverted using a U.V. laser focused to the cell body. After ~1 hour the spread of red Kaede is observed again.

(B) Upper panel: confocal reconstructions of wild-type L4 animal immediately after dendrotomy, green fluorescence 24 hours after injury and before photoconversion, red fluorescence before photoconversion and red fluorescence an hour after photoconversion of the cell-body. In the lower panel are illustrations. Red kaede passed into the distal area, meaning that the broken dendrite fused to the proximal part.

(C) A negative control showing L4 wild-type animal in which the primary branch did not regenerate within 24 hours. Proximal menorahs are fused (arrows), but it did not bridge the gap between the distal and proximal stumps (arrowheads). Indeed red kaede did not spread into the detached distal stump. The order of images is the same as described in **(B)**. Lightings point at injury sites, arrows point at fusion sites. Scale bars, 20 µm.

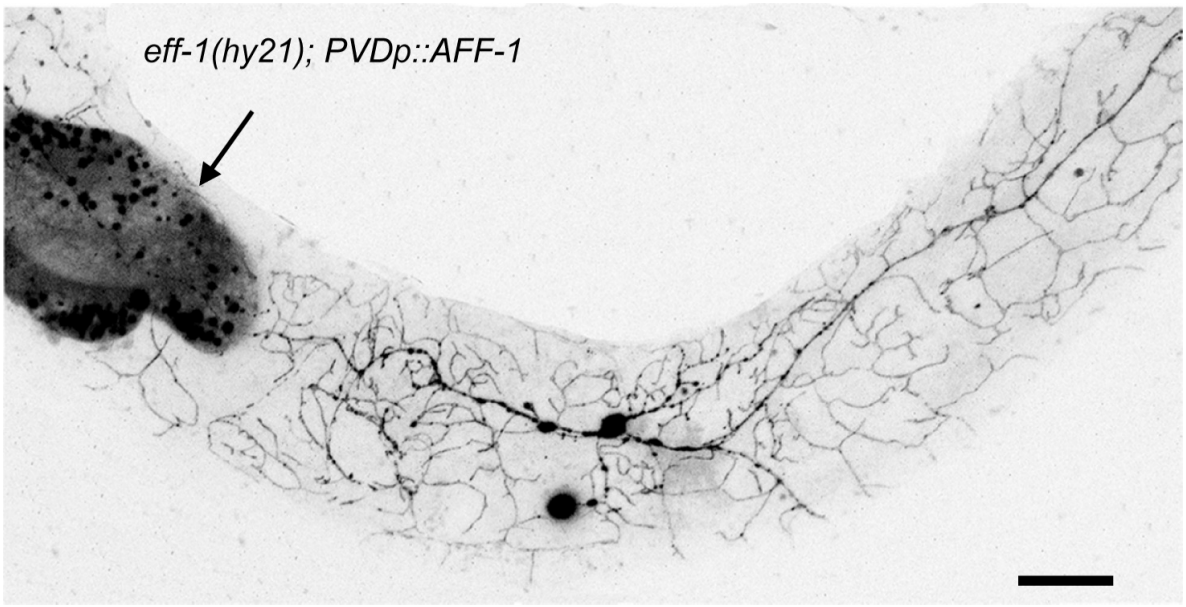

Figure 7-figure supplement 1.

AFF-1 does not retract PVD's dendrites. *eff-1(hy21)* animals expressing AFF-1 in the PVD (PVDp::AFF-1) show excess branching, similarly to *eff-1* mutants

Thus the fusogen AFF-1 cannot rescue *eff-1* loss-of-function phenotype when expressed in the PVD. Arrow points to hypodermal cells expressing GFP after ectopic PVD neurite-epidermal fusion. Scale bar, 10 μm.

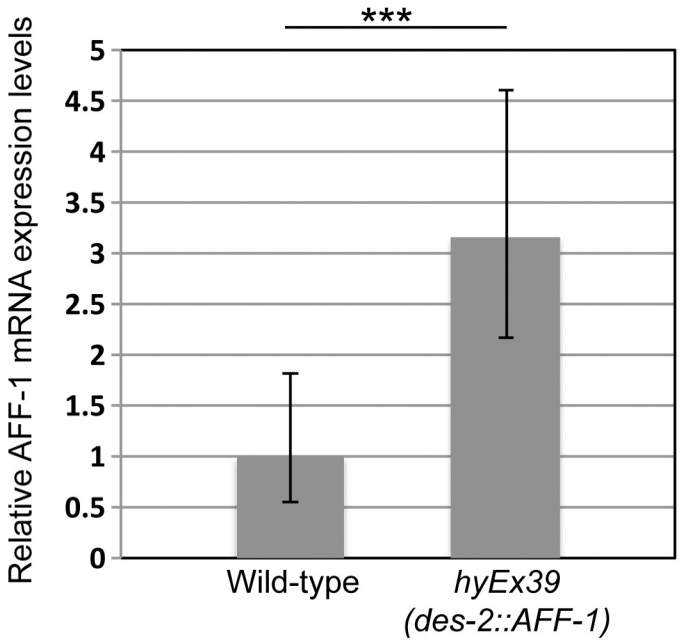

Figure 7-figure supplement 2.

Real-time RT-PCR analysis of AFF-1 mRNA expression in wild-type and transgenic worms over expressing AFF-1 in the PVD. Bar graph representing the fold changes of mRNA levels quantified by normalization to the *act-1* gene as an internal control. *p* value from *t* test ***$p<0.0001$.

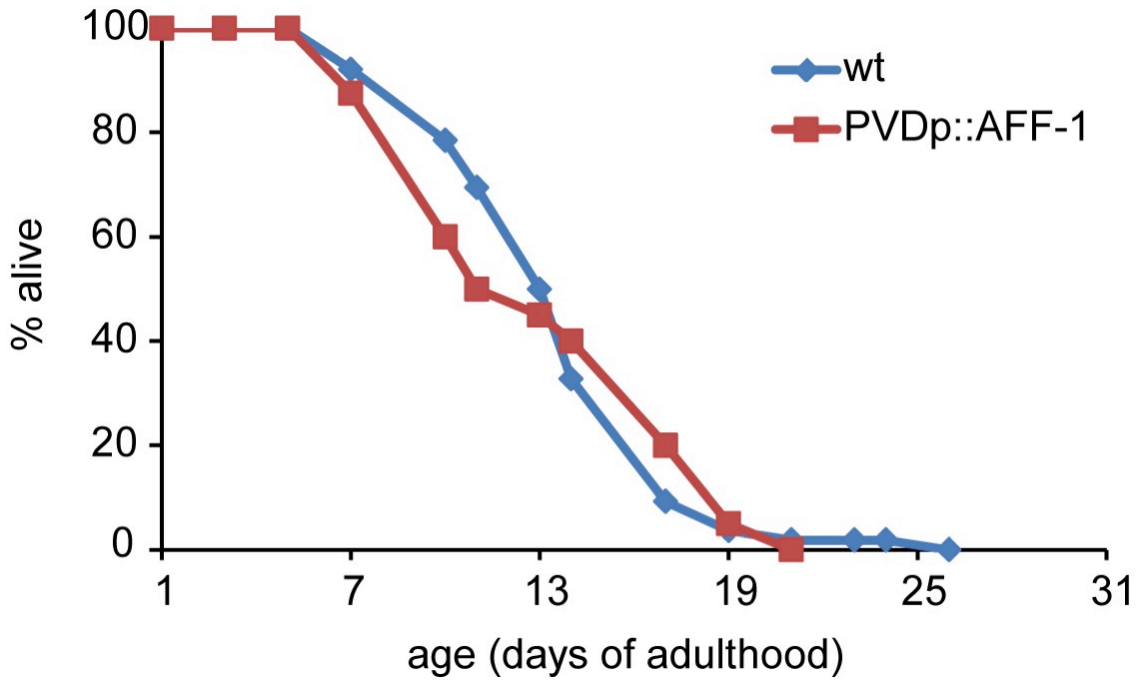

Figure 8-figure supplement 1.

AFF-1 overexpressing animals exhibit wild-type life-span

Life-span curve of wild-type (blue) and AFF-1 overexpression in the PVD (PVDp::AFF-1, red) . Median life-span is 14 days of adulthood for wild-types and 13 for PVDp::AFF-1 containing animals.

734

735 **Legends for movies**

736

737 **Movie S1. Dendritic plasticity of aged wild-type**

738 Inverted fluorescence confocal maximum intensity projections time lapse movie of wild-type
739 PVD marked with GFP at 5 days of adulthood. Some branches show dynamic growth and
740 retraction (arrow). The counter in this and other movies are in Hours: minutes.

741

742 **Movie S2. Young wild-types regenerate rapidly after dendrotomy**

743 Inverted fluorescence confocal maximum intensity projections time lapse movie of two L4
744 wild-type animals. PVD marked with Kaede. Both animals regenerated within 2 hours after
745 laser induced dendrotomy via menorah-menorah fusion (blue arrows). Red lightnings mark
746 the sites of injury.

747

748 **Movie S3. Kaede photoconversion confirms auto-fusion as part of regeneration**

749 Confocal time lapse movie of wild-type L4 worm expressing the photoconvertible protein
750 Kaede in the PVD. The 1ry branch of this worm was dendrotomized 24 hours prior to the
751 movie, then green kaede was photoconverted in the cell body, using U.V. laser (marked with
752 purple asterisk). In the left panel the red channel is seen, with red for the photoconverted
753 kaede protein traveling from the proximal part to the fused distal part (blue arrows). In the
754 right panel the green channel is shown. Injury site is indicated by yellow lightning. The
755 photoconverted red-Kaede was transferred to the distal part (top of the image) by menorah-
756 menorah fusion and there was no 1ry-1ry fusion.

757

758

759 **Movie S4. Adult wild-type responds slowly to injury**

760 Inverted fluorescence confocal maximum intensity projections time lapse movie of wild-type
761 animal at the age of 2 days of adulthood. PVD is marked by Kaede. There is neither
762 regeneration nor degeneration within the first 3 hours after cut. Red lightning points at injury
763 site.

764

765 **Movie S5. PVDp::AFF-1 L4 regenerates similarly to wild-type**

766 Inverted fluorescence confocal maximum intensity projections time lapse movie of
767 PVDp::AFF-1 (AFF-1 overexpression in the PVD) L4 nematode. The worm was injured and
768 imaged immediately after. In this movie, it rapidly regenerates (within 3 hours from cut) via
769 menorah-menorah fusion, as marked by blue arrows and by novel outgrowth that fuses to the
770 distal primary and by that bridges the gap (yellow arrow). Red lightning points to injury site.
771 Red arrowhead marks a menorah that degenerated during the movie.

772

773 **Movie S6. PVDp::AFF-1 5d old animal reconnects after cut**

774 Confocal time lapse movie of 5 days old PVDp::AFF-1 transgenic animal, beginning 5 hours
775 post injury. Growth is seen near site of dendrotomy. The primary branch grows toward the
776 distal primary and reconnects with it 10 hours after injury (blue arrows). After this time point
777 the worm was recovered and imaged 15 hours later (25 hours after cut), where regeneration
778 via novel outgrowth from 1ry to distal fragment of 1ry branch fusion and menorah-menorah
779 fusion is indicated by blue arrows. Red lightning points at injury site.